Inter-Symbol / Inter-Frame Interference in Time-Hopping Ultra Wideband Impulse Radio System

Anne-Laure Deleuze[1,2], Philippe Ciblat[2] and Christophe J. Le Martret[1]

[1]THALES Land and Joint Systems, 160 Bd de Valmy, B.P. 82, 92704 Colombes, France
Email: anne-laure.deleuze@fr.thalesgroup.com, christophe.le_martret@fr.thalesgroup.com
[2]École Nationale Supérieure des Télécommunications de Paris, 46, rue Barrault, 75013 Paris, France
Email: deleuze@enst.fr, philippe.ciblat@enst.fr

***Abstract*— A closed-form expression for the inter-symbol / inter-frame interference variance is derived in the context of a time-hopping ultra wideband impulse radio based system. This enables us to theoretically analyze on the performance the influence of the time-hopping codes, of the rake receiver number of fingers, and of the guard-time size. Simulations sustain our claims.**

I. Introduction

For several years, the Time-Hopping Ultra WideBand Impulse Radio (TH UWB-IR) based communication systems have received great attention, especially for short-range communication schemes. For these applications, a low-complexity, and a low-cost terminal is recommended.

In UWB systems with analog receiver implementations, it is conventional to use a rake receiver structure for simplicity. At the receiver, the energy captured grows with the rake receiver number of fingers (see *e.g.*, [1], [2]). This allows to take advantage of the temporal diversity brought by the UWB channel through multipaths. However, this temporal diversity gives rise to Inter Symbol / Inter Frame Interference (ISI / IFI) at the same time. For the same reason as for the energy capture phenomenon, the ISI / IFI energy collected at the receiver grows with the rake receiver number of fingers, which may degrade the performance. Thus, the important point is to understand how the signal to ISI / IFI ratio varies according to the number of fingers. This should help to determine the smallest number of fingers needed since it is a crucial parameter in the complexity design of the receiver. A possible way to mitigating the effect of the ISI / IFI is to resort to guard-time between frames as advocated in [3], and [4] at the expense of spectral efficiency. The effect of the number of fingers has been investigated by simulations in [1], [2], [5], [6], [7] and no studies have been done for the guard-time.

Thus, the main purpose of this paper is to obtain a closed-form expression of the ISI / IFI energy at the output of a rake receiver that shows the contribution of the Time-Hopping Codes (THC), the rake receiver number of fingers and the guard-time size on the ISI / IFI energy. This expression will be useful in adjusting the rake receiver parameters when designing practical systems.

The paper is organized as follows: in Section II, we introduce the TH UWB-IR based system as well as the propagation channel model. In Section III, we provide the original closed-form expression of the ISI / IFI power. Section IV is devoted to simulations. Conclusions are drawn in Section V.

II. System Model

We consider here a Pulse Amplitude Modulation (PAM) format but extension to pulse position modulation can be done similarly. The transmit signal of the user of interest takes the following form [3]:

$$s(t) = \sum_{i=-\infty}^{+\infty} d(\lfloor i/N_f \rfloor) w(t - iT_f - \tilde{c}(i)T_c), \qquad (1)$$

where N_c is the number of chips of duration T_c, N_f is the number of frames of duration $T_f := N_c T_c$, $w(t)$ is the pulse of duration $T_w \ll T_c$, $\lfloor x \rfloor$ is the integer-floor of x. The transmitted symbols $d(i) \in \{-1, 1\}$ are assumed to be independent and identically distributed (***i.i.d.***). The THC $\{\tilde{c}(i)\}_{i=0}^{N_f-1}$, whose values are drawn in $\{0, N_c - 1\}$, is assumed to be periodic of period N_f. In order to facilitate the derivations, we rewrite (1), by using the so-called developed time-hopping code $\{c(j)\}_{j=0}^{N_c N_f -1}$ deduced from the THC $\{\tilde{c}(i)\}_{i=0}^{N_f-1}$, as follows [8]:

$$c(j) = \begin{cases} 1 & \text{if } j = \tilde{c}(i) + iN_c,\ 0 \leq i \leq N_f - 1, \\ 0 & \text{otherwise.} \end{cases}$$

Thanks to the developed time-hopping code, (1) can be rewritten in the following way:

$$s(t) = \sum_{i=-\infty}^{+\infty} d(i) \sum_{j=0}^{N_c N_f - 1} c(j) w(t - iN_f T_f - jT_c).$$

One can remark that the transmit signal now only depends on the developed code linearly.

Since the ISI / IFI at the rake receiver output does only depend on the user of interest [9], we can consider here the single user case. Thus, after propagation through the multipath channel, the received signal can be expressed as follows:

$$r(t) = \sum_{k=1}^{N_p} A_k s(t-\tau_k) + n(t), \tag{2}$$

where A_k and τ_k are the amplitude and the delay of the k^{th} path respectively, and where N_p is the number of paths, and $n(t)$ is a zero-mean white Gaussian noise.

The channel model considered here is the conventional one established for UWB personal area network [10], [11], with one cluster. The amplitudes are zero-mean random variables given by $A_k = a_k \cdot e^{-\tau_k/2\gamma}$ with γ the ray decay factor, and $a_k = p_k \cdot \beta_k$ where $p_k \in \{-1,+1\}$ is an equi-likely binary random sequence and where β_k a log-normal random variable. The delays τ_k are independent Poisson random variables with parameter λ and as a consequence, the difference between two consecutive delays obeys an exponential distribution with parameter λ. We define $\sigma_a^2 := \mathbb{E}_a[a_k^2]$, and fourth-moment $\mu_a^4 := \mathbb{E}_a[a_k^4]$. We also put $I_k := \mathbb{E}_a[A_k^2] = \sigma_a^2 \cdot e^{-\tau_k/\gamma}$.

At the receiver, we consider a rake receiver that selects any subset $\mathscr{L}$ of the L_r paths (with $L_r \leq N_p$). Without loss of generality, the receiver demodulates the symbol $d(0)$ (which is assumed to be equal to 1). Then, the signal at the output of the rake receiver can be written as

$$z = \sum_{\ell \in \mathscr{L}} A_\ell \int_0^{N_f T_f} r(t+\tau_\ell) \times v(t) \mathrm{d}t, \tag{3}$$

where $v(t) := \sum_{j=0}^{N_c N_f -1} c(j) w(t - jT_c)$ is the receiver template. By putting (2) into (3) and defining $z' := z - \eta$ with η the filtered noise due to $n(t)$ contribution, we obtain:

$$z' = \sum_{\ell \in \mathscr{L}} \sum_{k=1}^{N_p} A_\ell A_k \times y_{k,\ell},$$

with:

$$y_{k,\ell} = \sum_{i=-\infty}^{+\infty} d(i) \sum_{j,j'=0}^{N_c N_f -1} c(j) c(j') r_{ww}(\Delta\tau_{k,\ell} + (j-j')T_c + iN_f T_f),$$

where

$$r_{ww}(s) := \int_{-\infty}^{+\infty} w(t) w(t-s) dt,$$

and

$$\Delta\tau_{k,\ell} := \tau_k - \tau_\ell.$$

Moreover, according to [9] and [12], the term $y_{k,\ell}$ can be simplified as follows:

$$\begin{aligned} y_{k,\ell} \; = \; & d(-Q^{k,\ell}) \big[\mathscr{C}^+(q^{k,\ell}) r_{ww}(\varepsilon^{k,\ell}) \\ + \; & \mathscr{C}^+(q^{k,\ell}+1) r_{ww}(\varepsilon^{k,\ell} - T_c)\big] \\ + \; & d(-Q^{k,\ell}-1) \big[\mathscr{C}^-(q^{k,\ell}) r_{ww}(\varepsilon^{k,\ell}) \\ + \; & \mathscr{C}^-(q^{k,\ell}+1) r_{ww}(\varepsilon^{k,\ell} - T_c)\big], \end{aligned}$$

where

$$\begin{aligned} \mathscr{C}^+(q) \; &:= \; \sum_{k=q}^{N_c N_f -1} c(k) c(k-q) \\ \mathscr{C}^-(q) \; &:= \; \sum_{k=0}^{q-1} c(k) c(k-q), \end{aligned}$$

and where the difference between two delays can be decomposed as follows

$$\Delta\tau_{k,\ell} = Q^{k,\ell} N_f T_f + q^{k,\ell} T_c + \varepsilon^{k,\ell},$$

with $Q^{k,\ell} = \lfloor (\Delta\tau_{k,\ell})/N_f T_f \rfloor$, $q^{k,\ell} = \lfloor (\Delta\tau_{k,\ell} - Q^{k,\ell} N_f T_f)/T_c \rfloor$, and the remainder $\varepsilon^{k,\ell} \in [0, T_c)$.

The term z' can be split into two terms $z' = z_1 + z_2$ with

$$z_1 \; := \; \sum_{\ell \in \mathscr{L}} A_\ell^2 \cdot y_{\ell,\ell}, \tag{4}$$

$$z_2 \; := \; \sum_{\ell \in \mathscr{L}} \sum_{\substack{k=1 \\ k \neq \ell}}^{N_p} A_\ell A_k \cdot y_{k,\ell}, \tag{5}$$

z_1 is the useful collected energy, and z_2 is the ISI / IFI.

In the following Section, we derive a closed-form expression of the averaged variance of the ISI / IFI denoted by:

$$V := \mathbb{E}_{a,d,\tau}[z_2^2].$$

III. Closed-form expression for the ISI / IFI variance

Firstly, we address the derivation of the ISI / IFI variance averaged over the amplitudes a_k and the symbols $\{d(i)\}$ given the delays τ_k. Since the amplitudes A_k are independent with zero-mean, and since the symbols $\{d(i)\}$ are *i.i.d.*, after tedious calculations, we obtain:

$$\begin{aligned} \mathbb{E}_{a,d}[z_2^2] = \sum_{\ell \in \mathscr{L}} \sum_{\substack{k=1 \\ k \neq \ell}}^{N_p} I_\ell I_k \Big(& \big[(\delta_{Q^{k,\ell}} \times \mathbb{1}_{k \in \mathscr{L}} + 1) \mathscr{C}^{+2}(q^{k,\ell}) \\ & + (\delta_{Q^{k,\ell}+1} \times \mathbb{1}_{k \in \mathscr{L}} + 1) \mathscr{C}^{-2}(q^{k,\ell})\big] \\ & \times r_{ww}^2(\varepsilon^{k,\ell}) \\ + \quad & \big[(\delta_{Q^{k,\ell}} \times \mathbb{1}_{k \in \mathscr{L}} + 1) \mathscr{C}^{+2}(q^{k,\ell}+1) \\ & + (\delta_{Q^{k,\ell}+1} \times \mathbb{1}_{k \in \mathscr{L}} + 1) \mathscr{C}^{-2}(q^{k,\ell}+1)\big] \\ & \times r_{ww}^2(\varepsilon^{k,\ell} - T_c)\Big), \end{aligned} \tag{6}$$

where $\mathbb{1}_{k \in \mathscr{L}}$ is equal to 1 when $k \in \mathscr{L}$ and 0 otherwise.

We now average (6) over the delays τ_k. From now, we only consider the partial rake receiver, *i.e.*, $\mathscr{L} = \{1, 2, \cdots, L_r\}$. Notice that the partial rake receiver fingers are associated with the first successive delays and not with the most energetic delays as done for the so-called selective rake receiver. Unlike the selective rake receiver, the choice of the partial-rake receiver enables us to derive a closed-form expression for the statistics of the encountered delays and consequently, for $\mathbb{E}_{a,d,\tau}[z_2^2]$.

From (6), we easily deduce that:

$$\mathbb{E}_{a,d,\tau}[z_2^2] \;=\; \sigma_a^4\Big[2\sum_{\ell=1}^{L_r}\sum_{k=\ell+1}^{L_r}\big(Y_1^{k,\ell}+\bar{Y}_2^{k,\ell}+Y_3^{k,\ell}+\bar{Y}_4^{k,\ell}\big) + \sum_{\ell=1}^{L_r}\sum_{k=L_r+1}^{N_p}\big(\bar{Y}_1^{k,\ell}+\bar{Y}_2^{k,\ell}+\bar{Y}_3^{k,\ell}+\bar{Y}_4^{k,\ell}\big)\Big], \quad (7)$$

where

$$\begin{aligned}
Y_1^{k,\ell} &:= \mathbb{E}_\tau\big[(\delta_{Q^{k,\ell}}+1)\cdot e^{-(\tau_\ell+\tau_k)/\gamma} \times\mathscr{C}^{+2}(q^{k,\ell})r_{ww}^2(\varepsilon^{k,\ell})\big],\\
\bar{Y}_1^{k,\ell} &:= \mathbb{E}_\tau\big[e^{-(\tau_\ell+\tau_k)/\gamma}\mathscr{C}^{+2}(q^{k,\ell})r_{ww}^2(\varepsilon^{k,\ell})\big],\\
\bar{Y}_2^{k,\ell} &:= \mathbb{E}_\tau\big[e^{-(\tau_\ell+\tau_k)/\gamma}\mathscr{C}^{-2}(q^{k,\ell})r_{ww}^2(\varepsilon^{k,\ell})\big],\\
Y_3^{k,\ell} &:= \mathbb{E}_\tau\big[(\delta_{Q^{k,\ell}}+1)\cdot e^{-(\tau_\ell+\tau_k)/\gamma} \times\mathscr{C}^{+2}(q^{k,\ell}+1)r_{ww}^2(\varepsilon^{k,\ell}-T_c)\big],\\
\bar{Y}_3^{k,\ell} &:= \mathbb{E}_\tau\big[e^{-(\tau_\ell+\tau_k)/\gamma}\mathscr{C}^{+2}(q^{k,\ell}+1)r_{ww}^2(\varepsilon^{k,\ell}-T_c)\big],
\end{aligned}$$

and

$$\bar{Y}_4^{k,\ell} := \mathbb{E}_\tau\big[e^{-(\tau_\ell+\tau_k)/\gamma}\mathscr{C}^{-2}(q^{k,\ell}+1)r_{ww}^2(\varepsilon^{k,\ell}-T_c)\big].$$

In the following, we only focus on the derivations of $Y_1^{k,\ell}$. The other terms can be derived in a similar way. By noticing that $\tau_k+\tau_\ell = 2\tau_\ell+\Delta\tau_{k,\ell}$ and that τ_ℓ is independent of $\Delta\tau_{k,\ell}$ as soon as $\ell<k$, we get

$$Y_1^{k,\ell} = X_1^{k,\ell}\times\widetilde{X}_1^{k,\ell},$$

with

$$X_1^{k,\ell} = \mathbb{E}_{\tau_\ell}[e^{-2\tau_\ell/\gamma}],$$

and

$$\widetilde{X}_1^{k,\ell} = \mathbb{E}_{\Delta\tau_{k,\ell}}[(\delta_{Q^{k,\ell}}+1)\mathscr{C}^{+2}(q^{k,\ell})e^{-\Delta\tau_{k,\ell}/\gamma} \times r_{ww}^2(\Delta\tau_{k,\ell}-Q^{k,\ell}N_fT_f-q^{k,\ell}T_c)].$$

One can easily check that τ_ℓ and $\Delta\tau_{k,\ell}$ have the following probability density functions

$$p_{\tau_\ell}(t) = \frac{\lambda^\ell}{(\ell-1)!}t^{\ell-1}e^{-\lambda t}\times\mathbb{1}_{t\geq 0},$$

and

$$p_{\Delta\tau_{k,\ell}}(t) = \frac{\lambda^{k-\ell}}{(k-\ell-1)!}t^{k-\ell-1}e^{-\lambda t}\times\mathbb{1}_{t\geq 0}.$$

Consequently we obtain that

$$X_1^{k,\ell} = \frac{\lambda^\ell}{(\ell-1)!}\int_0^{+\infty}t^{\ell-1}e^{-(\lambda+2/\gamma)t}dt = \left[\frac{\lambda}{\lambda+2/\gamma}\right]^\ell. \quad (8)$$

Finding a closed-form expression for $\widetilde{X}_1^{k,\ell}$ is more difficult and can be done in the following manner: let $t:=\Delta\tau_{k,\ell}$, $Q_t = Q^{k,\ell}$, $q_t = q^{k,\ell}$ and $\varepsilon_t = \varepsilon^{k,\ell}$. By splitting interval $[0,+\infty)$ into an infinite number of interval of length T_c and by using the fact that $Q_t = Q_{nN_fT_f} = n$ for $t\in[nN_fT_f,(n+1)N_fT_f)$ and $q_t = q_{n'T_c} = n'$ for $t\in[n'T_c,(n'+1)T_c)$ with n and n' two integers, one can see that $\widetilde{X}_1^{k,\ell}$ takes the following form

$$\widetilde{X}_1^{k,\ell} = \frac{\lambda^{k-\ell}}{(k-\ell-1)!}\sum_{n=0}^{+\infty}\sum_{n'=0}^{N_cN_f-1}\mathscr{C}^{+2}(n')(\delta_n+1)e^{-(\lambda+1/\gamma)(nN_fT_f+n'T_c)} \times\int_0^{T_c}(nN_fT_f+n'T_c+\varepsilon)^{k-\ell-1}e^{-(\lambda+1/\gamma)\varepsilon}r_{ww}^2(\varepsilon)\mathrm{d}\varepsilon.$$

Merging previous equation, and (8) into (7) leads to the final result:

$$\begin{aligned}
V \;=\; \sigma_a^4\sum_{n=0}^{+\infty}\sum_{n'=0}^{N_cN_f-1}&\big(\mathscr{C}^{+2}(n')+\mathscr{C}^{-2}(n')\big)\Phi_{N_p,L_r}(n,n')\\
&+\big(\mathscr{C}^{+2}(n'+1)+\mathscr{C}^{-2}(n'+1)\big)\Psi_{N_p,L_r}(n,n')\\
&+2\big((\delta_n+1)\mathscr{C}^{+2}(n')+\mathscr{C}^{-2}(n')\big)\Phi_{L_r,L_r}(n,n') \qquad (9)\\
&+2\big((\delta_n+1)\mathscr{C}^{+2}(n'+1)+\mathscr{C}^{-2}(n'+1)\big)\Psi_{L_r,L_r}(n,n').
\end{aligned}$$

with

$$\Phi_{N,L}(n,n') = e^{-(\lambda+1/\gamma)(nN_fT_f+n'T_c)} \times\sum_{\ell=1}^{L}\frac{1}{(\lambda+2/\gamma)^\ell}\sum_{k=\ell+1}^{N}\frac{\lambda^k}{(k-\ell-1)!} \times\int_0^{T_c}(nN_fT_f+n'T_c+\varepsilon)^{k-\ell-1}e^{-(\lambda+1/\gamma)\varepsilon}r_{ww}^2(\varepsilon)\mathrm{d}\varepsilon,$$

and

$$\Psi_{N,L}(n,n') = e^{-(\lambda+1/\gamma)(nN_fT_f+n'T_c)} \times\sum_{\ell=1}^{L}\frac{1}{(\lambda+2/\gamma)^\ell}\sum_{k=\ell+1}^{N}\frac{\lambda^k}{(k-\ell-1)!} \times\int_0^{T_c}(nN_fT_f+n'T_c+\varepsilon)^{k-\ell-1}e^{-(\lambda+1/\gamma)\varepsilon}r_{ww}^2(\varepsilon-T_c)\mathrm{d}\varepsilon.$$

The term $\Phi_{N,L}(n,n')$ can be simplified in the following way, when $N>L$,

$$\Phi_{N,L}(n,n') = \lambda e^{-(nN_fT_f+n'T_c)/\gamma}\sum_{\ell=1}^{L}\left(\frac{\lambda}{\lambda+2/\gamma}\right)^\ell \times\int_0^{T_c}e^{-\varepsilon/\gamma}\frac{\Gamma(N-\ell,\lambda(nN_fT_f+n'T_c+\varepsilon))}{\Gamma(N-\ell)}r_{ww}^2(\varepsilon)\mathrm{d}\varepsilon,$$

and, when $N=L$,

$$\Phi_{L,L}(n,n') = \lambda e^{-(nN_fT_f+n'T_c)/\gamma}\sum_{\ell=1}^{L-1}\left(\frac{\lambda}{\lambda+2/\gamma}\right)^\ell \times\int_0^{T_c}e^{-\varepsilon/\gamma}\frac{\Gamma(L-\ell,\lambda(nN_fT_f+n'T_c+\varepsilon))}{\Gamma(L-\ell)}r_{ww}^2(\varepsilon)\mathrm{d}\varepsilon,$$

with the incomplete Gamma function and the Gamma function respectively defined as

$$\Gamma(a,x) := \int_x^{+\infty}t^{a-1}e^{-t}\mathrm{d}t, \qquad a>0,$$

and

$$\Gamma(a) := \int_0^{+\infty} t^{a-1} e^{-t} \mathrm{d}t, \qquad a > 0.$$

The terms $\Psi_{N,L}(n,n')$ and $\Psi_{L,L}(n,n')$ take the following similar forms:

$$\Psi_{N,L}(n,n') = \lambda e^{-(nN_f T_f + n'T_c)/\gamma} \sum_{\ell=1}^{L} \left(\frac{\lambda}{\lambda+2/\gamma}\right)^{\ell}$$
$$\int_0^{T_c} e^{-\varepsilon/\gamma} \frac{\Gamma(N-\ell, \lambda(nN_f T_f + n'T_c + \varepsilon))}{\Gamma(N-\ell)} r_{ww}^2(\varepsilon - T_c)\mathrm{d}\varepsilon,$$

and, when $N = L$,

$$\Psi_{L,L}(n,n') = \lambda e^{-(nN_f T_f + n'T_c)/\gamma} \sum_{\ell=1}^{L-1} \left(\frac{\lambda}{\lambda+2/\gamma}\right)^{\ell}$$
$$\int_0^{T_c} e^{-\varepsilon/\gamma} \frac{\Gamma(L-\ell, \lambda(nN_f T_f + n'T_c + \varepsilon))}{\Gamma(L-\ell)} r_{ww}^2(\varepsilon - T_c)\mathrm{d}\varepsilon.$$

Simplifications can be done when considering that number of paths N_p goes to infinity (*i.e.*, the asymptotic regime), which actually corresponds to reality (the amplitudes going down to zero due to exponential decay) we put $\Phi_{\infty,L_r}(n,n') := \lim_{N_p\to\infty} \Phi_{N_p,L_r}(n,n')$ and $\Psi_{\infty,L_r}(n,n') = \lim_{N_p\to\infty} \Psi_{N_p,L_r}(n,n')$ given by

$$\Phi_{\infty,L_r}(n,n') = e^{-(nN_f T_f + n'T_c)/\gamma} \frac{\lambda^2\gamma}{2}\left[1 - \left(\frac{\lambda}{\lambda+2/\gamma}\right)^{L_r}\right]$$
$$\times \int_0^{T_c} e^{-\varepsilon/\gamma} r_{ww}^2(\varepsilon)\mathrm{d}\varepsilon,$$
$$\Psi_{\infty,L_r}(n,n') = e^{-(nN_f T_f + n'T_c)/\gamma} \frac{\lambda^2\gamma}{2}\left[1 - \left(\frac{\lambda}{\lambda+2/\gamma}\right)^{L_r}\right]$$
$$\times \int_0^{T_c} e^{-\varepsilon/\gamma} r_{ww}^2(\varepsilon - T_c)\mathrm{d}\varepsilon,$$

respectively. Notice that the terms $\Phi_{L_r,L_r}(n,n')$ and $\Psi_{L_r,L_r}(n,n')$ do not change in asymptotic regime since L_r is a fixed finite number. One can remark that $\Phi_{1,1}(n,n') = \Psi_{1,1}(n,n') = 0$ for a one-finger rake receiver. In the following we put:

$$V_\infty := \lim_{N_p\to\infty} V.$$

The rigorous analysis of the closed-form expression V_∞ versus various parameters (code optimization, channel parameters, rake receiver number of fingers) is not easy. Nevertheless we are able to interpret roughly this expression as follows.

We may remark that the terms $\Phi_{\infty,L_r}(n,n')$, $\Psi_{\infty,L_r}(n,n')$, $\Phi_{L_r,L_r}(n,n')$, and $\Psi_{L_r,L_r}(n,n')$ decrease exponentially with respect to n and n'. Consequently in order to get the expression (9) (with $N_p \to \infty$) as small as possible, we need to prevent collisions for small n and n'. Therefore the optimal codes (which minimize ISI / IFI) offer null correlations for small lags.

The channel parameters have also an impact on the ISI / IFI. The parameter λ refers to the path density and the parameter γ is associated with the path decaying speed. For instance, the larger γ is, the longer the channel impulse response is. By inspecting properly the expressions of $\Phi_{\infty,L_r}(n,n')$, $\Psi_{\infty,L_r}(n,n')$, $\Phi_{L_r,L_r}(n,n')$, and $\Psi_{L_r,L_r}(n,n')$ we note that the inverse of γ appears in the exponential factor. Consequently, the smaller γ is, the less the ISI / IFI variance is. This last statement is in agreement to the fact that the channel length (and so the ISI / IFI) decreases when γ decreases. Moreover the ISI / IFI variance is quasi-proportionnal to λ. Therefore the less λ is, the less the ISI / IFI variance is. This fact can be explained as follows: if λ is small, then the number of paths is also small, and thus the rake receiver (for fixed L_r) performs better which implies a smaller ISI / IFI variance.

We suspect that the codes optimization does not strongly depend on L_r. Indeed in the first two terms of the Right Hand Side (RHS) of expression (9) (with $N_p \to \infty$), the term $(1-(\lambda/(\lambda+2/\gamma))^{L_r})$ can be factorized and then the weighted sum of the correlation does not depend on L_r anymore. Furthermore, we have observed that the last two terms of the RHS of expression (9) are numerically weaker than the two first terms. This fact will be supported by simulation (cf. Fig. 2).

Let $U := \mathbb{E}_{a,\tau}[z_1^2]$ denotes the useful captured energy at the rake receiver output. From (4) the computation gives:

$$\begin{aligned} U &= N_f^2 r_{ww}^2(0)\lambda\gamma\left[\frac{\mu_a^4}{2} + \lambda\gamma + \left(\frac{\lambda}{\lambda+2/\gamma}\right)^{L_r}\right. \\ &\times \left.\left(\lambda\gamma + 2 - \frac{\mu_a^4}{2}\right) - 2\left(\frac{\lambda}{\lambda+1/\gamma}\right)^{L_r}(1+\lambda\gamma)\right]. \end{aligned}$$

IV. SIMULATIONS

The UWB-IR system is obtained by setting $N_f = 3$, $N_c = 10$, $T_c = 5$ ns, and $T_f = 50$ ns. The pulse $w(t)$ is designed such that its spectrum fits well the shape of the FCC spectral mask [13]. For practical purpose, the pulse (with unitary energy) is truncated with the duration $T_w = 1$ ns.

As for the propagation channel, we have considered the statistical parameters $\lambda = 0.1\,\mathrm{ns}^{-1}$, and $\gamma = 200\,\mathrm{ns}$. Notice that these channel parameters are different from those of [11]. In contrast with [11], the considered channel generates a non-negligible ISI / IFI. Indeed, by inspecting one realization of the channel plotted in Fig. 1, we see that the maximum delay spread is around 750 ns which is much greater than one symbol duration $T_s := N_f N_c T_c = 150$ ns. In the sequel, for each curve, $10,000$ Monte-Carlo trials are run.

In Fig. 2, we display U/V_∞ versus L_r for any THC. We have highlighted the best code for $L_r = 1$ and the mean-value over all the codes. We remark that the best code for $L_r = 1$ still offers good performance even for large L_r.

In Fig. 3, we have plotted the Average Error Probability (AEP), $\bar{P}_e$, derived as in [14] versus the average received bit energy to noise ratio ($\bar{E}_b/N_0$) for the best and the worst codes associated with three reasonable values of L_r ($L_r = 1$, $L_r = 3$ and $L_r = 5$). The best (resp. worst) code stands for the code which minimizes (resp. maximizes) the term V_∞. As the gap between the minimum and the maximum of V_∞ is small for $L_r = 1$ and $L_r = 3$, the gap in terms of error probability exists but remains small. Nevertheless the choice of the best

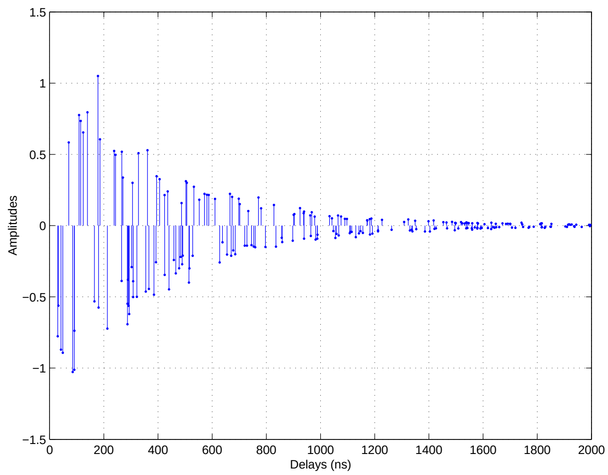

Fig. 1. One channel realization, $\lambda = 0.1\,\mathrm{ns}^{-1}$ and $\gamma = 200$ ns.

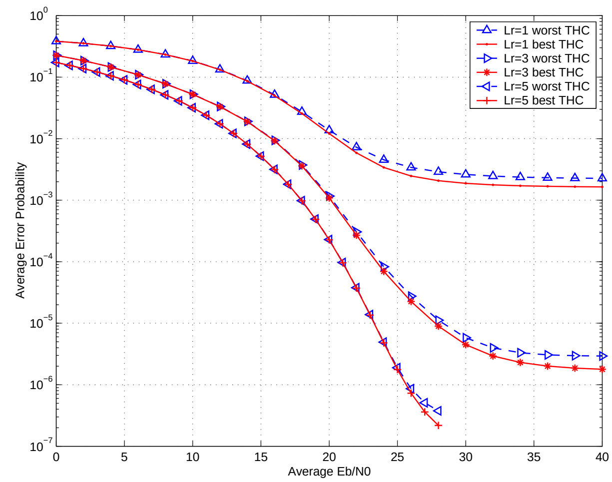

Fig. 3. $\bar{P}_e$ versus $\bar{E}_b/N_0$ for $L_r = 1$, $L_r = 3$ and $L_r = 5$.

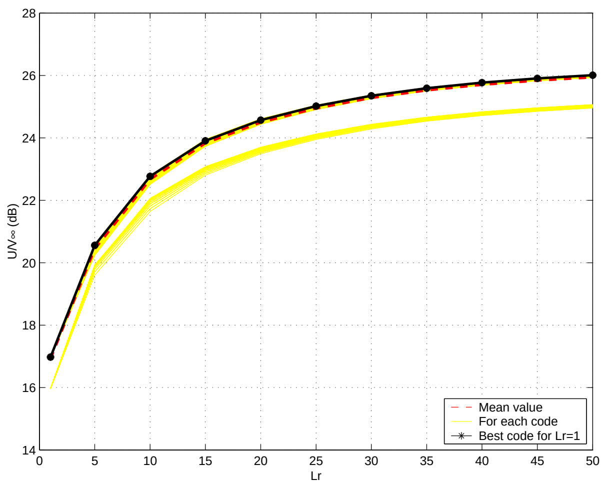

Fig. 2. U/V_∞ versus L_r for any code.

code enables us to improve slightly the performance. In order to obtain reasonnable performance without coding (AEP $\approx 10^{-3}$ or 10^{-5}), we observe that we do not need to choose large rake receiver number of finger. More precisely, in practice, it is not useful to select L_r reaching the floor in Fig. 2.

We now move on the analyze of the guard-time size on the performance. The guard-time is built by adding N_g empty chips. Consequently the new frame duration is $T_f = (N_g + N_c)T_c$. The guard-time duration is denoted by $T_g := N_g T_c$. In Fig 4, we have plotted U/V_∞ versus T_g for $L_r = 1$ and $L_r = 3$ and by selecting the THC which minimizes V_∞.

Surprisingly, when T_g becomes large, U/V_∞ does not tend towards infinity but towards a deterministic floor. Indeed the ISI / IFI does not vanish since it remains a collision between both non-empty chips of the same frame shifted by a delay belonging to $[-T_c, T_c]$. This residual interference can be deduced from (9) by keeping only the terms associated with $n = 0$ and $n' = 0$ and is equal to:

$$\sigma_a^4 N_f^2 \Big[4\Phi_{L_r,L_r}(0,0) + \Phi_{\infty,L_r}(0,0) \Big].$$

We remark that the residual interference is independent of the codes.

Fig. 4 may enable us to design appropriately the system. For instance, the guard-time size can be $T_g \approx 75$ ns which corresponds to a 3 dB loss with respect to the optimal value of U/V_∞. We will see that this choice is relevant in term of average error probability (cf. Fig. 5). As a conclusion, the guard-time size does not need to maximize U/V_∞, and it can be chosen smaller than expected.

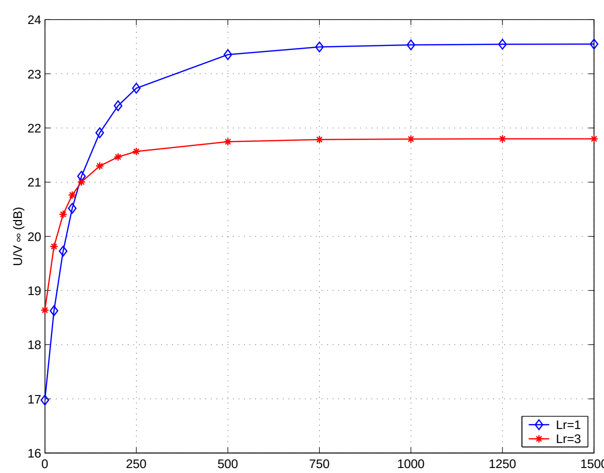

Fig. 4. U/V_∞ versus T_g for $L_r = 1$ and $L_r = 3$.

In Fig. 5, the average error probability $\bar{P}_e$ is computed versus $\bar{E}_b/N_0$ for various values of T_g. We set $L_r = 1$. For each point, we have selected the THC which minimizes V_∞. We observe that the performance slightly improves when the guard-time size grows. As mentioned in Fig. 4, the performance with respect to T_g rapidly reaches the optimal value. And this figure sustains the previous choice $T_g = 75$ns.

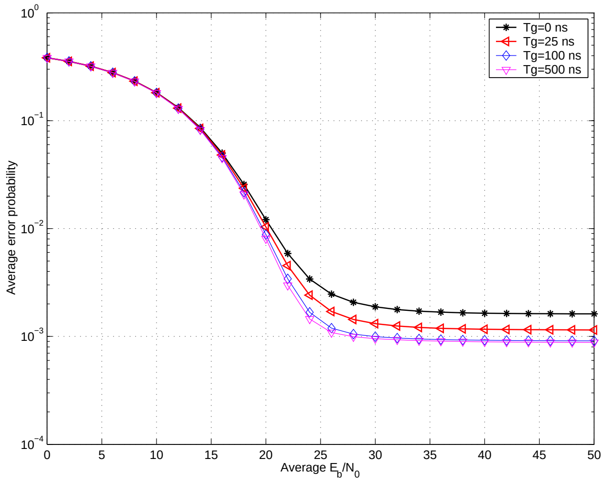

Fig. 5. $\bar{P}_e$ versus $\bar{E}_b/N_0$ for different values of T_g.

One can remark that there does not exist obvious link between U/V_∞ and the average probability $\bar{P}_e$. Actually there is no closed-form expression between both quantities because of the non-gaussianity of the ISI / IFI. In Figs. 6 and 7, we have plotted the Probability Density Functions (PDF) of z_2 when $L_r = 1$ and $L_r = 3$ respectively. As benchmark, the gaussian PDFs with the same variance have also been displayed. Additionally, the normalized kurtosis (which is equal to zero for Gaussian PDF) has been computed for z_2 and is equal to 13.75 (resp. 13.86) for $L_r = 1$ (resp. $L_r = 3$).

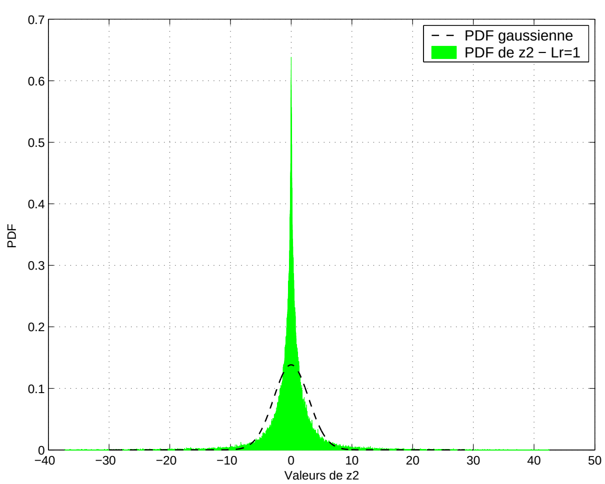

Fig. 6. PDF of z_2 and Gaussian PDF with same variance ($L_r = 1$)

V. Conclusion

In this paper, we provided a closed-form expression for the ISI / IFI power at the output of a partial rake receiver in a realistic UWB channel model. Then we remarked that the performance can be slightly improved by choosing carefully the time-hopping code and the guard-time size.

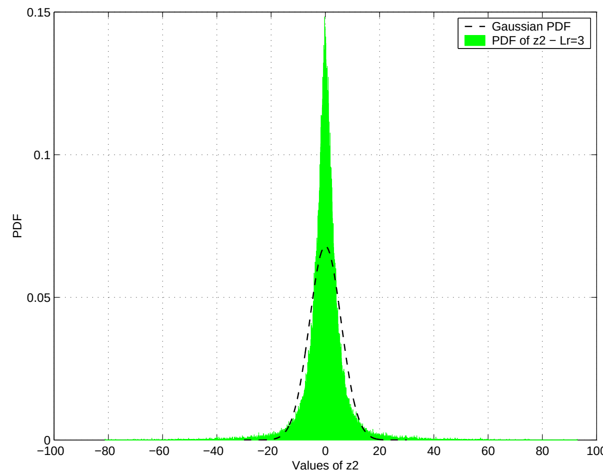

Fig. 7. PDF of z_2 and Gaussian PDF with same variance ($L_r = 3$)

References

[1] M. Z. Win and R. A. Scholtz, “On the energy capture of ultrawide bandwidth signals in dense multipath environments,” *IEEE Communications Letters*, vol. 2, no. 9, pp. 245–247, Sept. 1998.

[2] A. Rajeswaran, V. Srinivasa Somayazulu, and J. R. Foerster, “Rake performance for a pulse based UWB system in a realistic UWB indoor channel,” in *Proc. IEEE International Conference on Communications*, no. 1, Anchorage, USA, May 2003, pp. 2879–2883.

[3] M. Z. Win, and R. A. Scholtz, “Ultra-wide bandwidth time-hopping spread-spectrum impulse radio for wireless multiple-access communications,” *IEEE Trans. on Communications*, vol. 48, no. 4, pp. 679-691, April 2000.

[4] F. Ramírez-Mireles, “Error probability of ultra wideband SSMA in a dense multipath environment,” in *Proc. of the Milcom Conf.* , vol. 2, Anaheim, CA, USA, pp. 1081-1084, Oct. 2002.

[5] M. Z. Win and Z.A. Kostic, "Virtual path analysis of selective receiver in dense multipath channels," *IEEE Communications Letters*, vol. 3, no. 11, pp. 308–310, Nov. 1999.

[6] Y. Ishiyama and T. Ohtsuki, "Performance comparison of UWB-IR using rake receiver in UWB channel models," *International Workshop on Ultra Wideband Systems (UWBST/IWUWBS)*, pp. 226-230, May 2004.

[7] D. Cassioli, M. Z. Win, F. Vatalaro and A. F. Molish, “Performance of low-complexity rake reception in a realistic UWB Channel,” in *Proc. IEEE International Conference on Communications*, no. 2, New York, USA, May 2002, pp. 763–767.

[8] C. J. Le Martret, and G. B. Giannakis, “All-Digital impulse radio for wireless cellular systems,” *IEEE Trans. on Communications*, vol. 50, no. 9, pp. 1440-1450, Sept. 2002.

[9] A.-L. Deleuze, C. J. Le Martret and P. Ciblat, "Time-hopping code characterization for multi-user interference mitigation in ultra wide band impulse radio," Thirty-Eighth Asilomar Conference on Signals, Systems and Computer, Pacifi c Grove, CA, USA, Nov. 2004.

[10] A. A. M. Saleh, and R.A. Valenzuela, “A statistical model for indoor multipath propagation,” *IEEE Journal on Selected Areas in Communications*, vol. SAC-5, no. 2 pp. 128-137, Feb. 1987.

[11] A. F. Molish, J. R. Foerster, and M. Pendergrass, “Channel models for ultrawideband personal area networks,” *IEEE Wireless Communications*, vol. 10, Dec. 2003.

[12] C. J. Le Martret, A.-L. Deleuze, and P. Ciblat, "Optimal Time-Hopping Code Criterion for Multi-User Interference Mitigation in Ultra-Wide Bandwidth Impulse Radio," *Accepted for publication to IEEE Trans. on Wireless Communications*, Mar. 2005.

[13] Federal Communication Commission, “Revision of Part 15 of the commission’s rules regarding ultra-wideband transmission systems, fi rst Report and Order,” FCC, Feb. 2002.

[14] G. Durisi, and S. Benedetto, “Performance evaluation of TH-PPM UWB systems in the presence of multiuser interference,” *IEEE Communications Letters*, vol. 7, no. 5, pp. 224-226, May 2003.